

See discussions, stats, and author profiles for this publication at: <https://www.researchgate.net/publication/273768538>

Densely Packed Perylene Layers on the Rutile TiO₂ (110)-(1 × 1) Surface

ARTICLE *in* THE JOURNAL OF PHYSICAL CHEMISTRY C · MARCH 2015

Impact Factor: 4.77 · DOI: 10.1021/acs.jpcc.5b00851

READS

44

8 AUTHORS, INCLUDING:



José Ignacio Martínez
Spanish National Research Council
103 PUBLICATIONS 1,038 CITATIONS

[SEE PROFILE](#)



Valeria Lanzilotto
Uppsala University
22 PUBLICATIONS 123 CITATIONS

[SEE PROFILE](#)



Javier Méndez
Instituto de Ciencia de Materiales de Madrid
75 PUBLICATIONS 1,628 CITATIONS

[SEE PROFILE](#)



Maria Francisca López
Spanish National Research Council
108 PUBLICATIONS 1,908 CITATIONS

[SEE PROFILE](#)

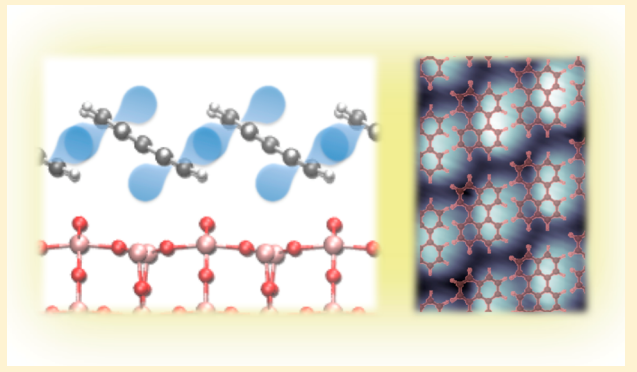
Densely Packed Perylene Layers on the Rutile $\text{TiO}_2(110)$ - (1×1) Surface

Gonzalo Otero-Irurueta,^{†,§} José I. Martínez,[†] Giacomo Lovat,[‡] Valeria Lanzilotto,^{‡,⊥} Javier Méndez,[†] María F. López,[†] Luca Floreano,[‡] and José A. Martín-Gago*,[†]

[†]ESISNA-Group, Department of Surfaces, Coatings & Molecular Astrophysics, Institute of Materials Science of Madrid (ICMM-CSIC), Sor Juana Inés de la Cruz 3, E-28049 Madrid, Spain

[‡]Laboratorio TASC, CNR-IOM, Basovizza SS-14, Km 163.5, I-34149 Trieste, Italy

ABSTRACT: We have studied the interaction of perylene, a prototypical organic molecule, on the $\text{TiO}_2(110)$ - (1×1) surface at different surface coverages by an adequate combination of ultrahigh vacuum STM and UPS techniques, together with accurate “many-body” corrected *ab initio* calculations. We show that the molecular coupling and adsorption configuration strongly depend on the coverage. At the submonolayer coverage, the interaction is dominated by the van der Waals substrate attraction, which keeps the molecules in the troughs between adjacent oxygen rows. At this low-coverage regime no additional interaction is detected among the molecules, which rather behave like a 2D gas. When the coverage approaches the saturation of the first layer, a *side-to-side* molecular attraction sets in, which is shown to be mediated by a lateral intermolecular hybridization.



1. INTRODUCTION

The study of the interaction between organic molecules and metal oxide surfaces is attracting considerable attention due to the wide range of possible applications like photovoltaics, gas sensing or catalysis, to name just a few.^{1–3} A deep and detailed understanding of the organic molecule/substrate interaction at the nanoscale is essential in order to include in this list nanoelectronic technology as another real application.^{4,5} To this aim, the surface of titanium dioxide provides suitable conditions for the use of surface experimental techniques. First, TiO_2 is a wide-band gap semiconductor, with a conductivity that can be enhanced by reducing the crystal upon thermal annealing. This allows the possibility of performing surface characterization techniques requiring electron emission and charge transport. On the other hand, the $\text{TiO}_2(110)$ surface provides an anisotropic template consisting of alternating bridging oxygen rows and 5-fold coordinated Ti^{4+} rows, making possible different adsorption geometries for different organic molecules.^{6,7} It is important to take into account that the final molecule/substrate orientation is a key parameter for determining the interaction nature at the interface.⁸

In the last years, the adsorption mechanisms of different organic molecules on the $\text{TiO}_2(110)$ surface have been a burgeoning matter of research.^{1,9–12} The possibility of selecting organic molecules with different size and shape is one of the most appealing issues for organic electronics. For this reason, contrasting species, ranging from highly symmetric C_{60} molecules,¹³ to planar molecules, and partial rounded nano-

domes ($\text{C}_{60}\text{H}_{30}$),¹⁴ have been studied on the $\text{TiO}_2(110)$ surface.

However, most of the recent works have been devoted to understand the interaction of planar molecules with the surface thanks to the efficient templating effect of the substrate anisotropy. Polycyclic aromatic hydrocarbons (PAHs) mostly adsorb with their major axis oriented parallel to the substrate atomic rows.^{15,16} The molecular plane results to be tilted-off of the surface by an angle γ that is usually dictated by the balance between the substrate attraction and the intermolecular coupling.^{17,18} The average tilt angle of the molecular overlayer can be measured by using some surface techniques, such as polarization dependent NEXAFS.¹⁹ Thus, for pentacene molecules adsorbed on the $\text{TiO}_2(110)$ surface, previous experiments showed a 25° tilt angle with their long axis parallel to the [001] surface direction, and adsorption sites on the 5-fold coordinated Ti rows.¹⁷ Pentacene molecules are found to be physisorbed on the surface and coupled *side-to-side* into long stripes, whereas the *head-to-head* repulsive interaction controls the spacing between the stripes.

On the other hand, different perylene derivatives have shown different structural configurations due to the interaction that is originated between the substrate and the chemical constituents of the molecules. Thus, in the case of PTCDA two regimes, physisorbed and chemisorbed, have been reported as a function

Received: January 27, 2015

Revised: March 18, 2015



ACS Publications

© XXXX American Chemical Society

A

DOI: 10.1021/acs.jpcc.5b00851
J. Phys. Chem. C XXXX, XXX, XXX–XXX

of the molecular coverage.²⁰ At low coverages, the molecules absorb flat with their long axis aligned along the [001] direction. Increasing the coverage toward the monolayer regime a *c*(2 × 6) phase of PTCDA is generated, where the molecules are bent onto the surface due to dispersion interactions. Contrastingly, in the case of PTCDI adsorbed on TiO₂(110) the molecules aggregate into compact (1 × 5) commensurate islands (with a tilt angle of 35°)²¹ due to the interplay among multiple interactions such as van der Waals attraction between neighboring molecules and between molecules and substrate, $\pi-\pi$ and $\sigma-\pi$ intermolecular coupling, chemical interaction between molecules and substrate, as well as head to tail chemical interaction (hydrogen bonding).²²

The identification of the weight of each specific interaction is fundamental to understand the different behavior of the electronically similar PTCDI and PTCDA derivatives, most importantly, it will give useful indications for the synthesis or selection of alternative derivatives in order to highlight specific molecular functionalities on this substrate. In this regard, perylene is the benchmark to disentangle the van der Waals, $\pi-\pi$ and $\sigma-\pi$ interactions associated with the common perylenic core of its derivatives. In order to fully explore the interaction between perylene molecules and this dielectric substrate, an adequate combination of experiments and first-principles calculations has been carried out. In this work, we show that the adsorption geometry highly depends on the coverage, where the molecules are axially tilted off the surface and van der Waals interactions are found to play a crucial role in the stabilization of the system. In particular, the intermolecular coupling is found to be relatively weaker than for pentacene, and an intermolecular correlation only sets in at the completion of the first wetting layer.

2. METHODS

2.1. Experimental Section. The STM experiments were carried out in an ultra-high vacuum (UHV) system with a base pressure of 1×10^{-10} mbar, equipped with a room-temperature scanning tunneling microscope (STM) and low-energy electron diffraction optics (LEED). WSxM software was used for data acquisition and analysis.²³

We performed low temperature ultraviolet photoemission spectroscopy (UPS) measurements of the valence band with a He discharge lamp installed at the HASPES end-station of the ALOISA beamline (Elettra Synchrotron, Trieste, Italy), where the perylene deposition could be monitored in real time and simultaneously by He atom scattering and X-ray photoemission, XPS.²⁴

The TiO₂(110) substrate was prepared by the standard procedure of repeated cycles of argon sputtering and annealing at 1100K in order to obtain the atomically flat 1 × 1 surface termination. STM and LEED were used for checking the quality of the sample previous to the molecular deposition. Perylene molecules (Sigma-Aldrich, sublimed grade, purity >99.5%) were first outgassed at an evaporation rate larger than that used to grow the molecular film. We used low deposition rates on the samples, typically in the range of 10–30 min/ML.

2.2. Theoretical Section. **2.2.1. Computational Details.** As a first consideration, it is worthwhile to remark that there is strong evidence that van der Waals (vdW)—or dispersion forces—play a paramount role in the adsorption mechanism of aromatic molecules on metal and oxide surfaces.^{14,25} On this basis, the important role of dispersion forces in the perylene/TiO₂(110) may lead, in comparison with non-vdW DFT

calculations, to a significant increase of the adsorption energies and distances, to an improved description of the intermolecular interaction at high coverage regime, and, what is even more relevant, to non-negligible geometric distortions of both the organic molecule and the substrate. Thus, a direct comparison between experiments and theory can only be reliable if an adequate theoretical vdW implementation to the conventional DFT is included.

In order to investigate the structural and electronic properties of both the different structural perylene/TiO₂(110) configurations obtained at different coverages (dilute and close-packed) we have used three different atomistic simulation packages: (i) the accurate plane-wave code PWSCF²⁶ is used for the characterization and optimization of the atomic configurations, by accounting van der Waals forces; (ii) the YAMBO code²⁷ is used to effectively include “many-body” corrections: to properly account for self-interaction energy and excitonic effects; and, finally, (iii) the efficient localized basis set code FIREBALL²⁸ is used for the theoretical STM-imaging calculations. Technical details concerning the mentioned approaches have been widely explained in detail elsewhere (see refs 26–28 and references therein).

Therefore, as starting point, different atomic geometries have been fully relaxed by means of DFT-based calculations by including dispersion forces within the DFT+D approach²⁹ as implemented in the PWSCF code.²⁶ For this purpose, we have used the revised version of the generalized gradient corrected approximation of Perdew, Burke, and Ernzerhof (rPBE),³⁰ and an empirical efficient vdW R^{-6} correction to add dispersive forces to conventional density functionals—see details in refs 29 and 31 and references therein. The ion–electron interaction is modeled by ultrasoft pseudopotentials,³² and the one-electron wave functions are expanded in a basis of plane-waves, with energy cutoffs of 400 and 500 eV for the kinetic energy and for the electronic density, respectively.

2.2.2. Many-Body Corrections. On the other hand, standard DFT calculations of electronic structure have well-known limitations, due to the approximate description of exchange and correlation effects between the electrons, such as the incorrect asymptotic behavior of the XC potential and the underestimation of the magnitude of the electronic energy gap in semiconductors.³³ A similar error can be expected for the gap between occupied and unoccupied electronic states (HOMO–LUMO gap) in finite clusters, nanoparticles³⁴ and organic molecules on metal/oxide interfaces,^{35,36} which is the present case. These errors could affect the energies of the excited electronic states, and thus to other related quantities such as the band structure, the photoabsorption spectrum, the STM currents and the electron–phonon coupling. For this reason, we have corrected the standard DFT electronic structure using many-body perturbation theory. We have calculated the many-body corrections by combining two different techniques: (a) quasiparticle corrections have been calculated within the G_0W_0 formalism (Green-function screened-interaction approach)^{37,38} to account for the exchange–correlation self-energy; and (b) the Bethe–Salpeter equation (BSE)^{34,39,40} where the quasiparticle G_0W_0 approach is further corrected to account for excitonic effects (electron–hole interaction) in the unoccupied and excited states. These GW+BSE calculations, based on the DFT band structure obtained using the PWSCF code, have been carried out with the YAMBO package.²⁷

Once the (GW+BSE)-corrected molecule band gap is obtained, the effects of the self-interaction energy and metal

dynamical polarization response on the interface electronic structure are included in our FIREBALL calculations in a practical and simplified way by introducing for each molecule a scissor operator $O^{scissor} = (U/2)\sum_{\langle\mu\nu\rangle}\{|\mu_i\rangle\langle\mu_i| - |\nu_i\rangle\langle\nu_i|\}$, with $|\mu_i\rangle$ and $|\nu_i\rangle$ being the empty (occupied) orbitals of the isolated molecule (with the actual geometry of the molecule on the surface). The charging energy for each perylene molecule, U , is taken from the (GW+BSE)-corrected molecule band gap. In a similar way, we also introduce a rigid shift (by ε_0) of the molecular levels of the perylene by means of a shift operator $O^{shift} = \varepsilon_0\sum_{\langle\beta\rangle}|\beta\rangle\langle\beta|$, with $|\beta\rangle$ being the orbitals for the isolated molecule. Using this operator we can fix, in our local-orbital DFT calculations, the *initial* energy level alignment between the perylene molecule and the $\text{TiO}_2(110)$ surface according to the experimental spectroscopic information. It is important to remark that these theoretical strategies have demonstrated to yield a widely improved description of the electronic structure of molecules on metals and oxides, in order to accurately obtain related quantities, such as density of state (DOS) profiles, charge transfers, band diagrams, and STM tunnel currents, among many others.^{14,41,42}

2.2.3. Theoretical STM Imaging. To conclude the theoretical framework description, once the electronic structure has been adequately corrected, theoretical STM calculations have been performed for all the perylene/ $\text{TiO}_2(110)$ configurations considered in this study, to be compared with the experimental evidence. In order to obtain accurate STM images and tunnelling currents, we used an efficient STM theoretical simulation technique that includes a detailed description of the electronic properties of both the tip and the sample.

Using this technique, based on a combination of a Keldysh Green's function formalism and local orbital density functional theory (DFT),^{43,44} we split the system into sample and tip, where the samples here are the different perylene/ $\text{TiO}_2(110)$ configurations tested. In these calculations we have assumed to simulate the scanning with a W-tip formed by 5 atoms (one of them in the apex) attached to an extended W(100)-crystal. Within this approach, in the tunnelling regime at low temperature, the STM current is given by^{43,44}

$$I = \frac{4\pi e^2}{\hbar} \int_{E_F}^{E_F+eV_s} d\omega \text{Tr}[T_t \rho_{ss}(\omega) T_{st} \rho_{tt}(\omega - eV)] \quad (1)$$

where V_s is the surface voltage, ρ_{tt} and ρ_{ss} are the density of states (DOS) matrices—in the local orbital basis—associated with the tip and sample, while T_{ts} and T_{st} are the local orbital Hamiltonian matrices coupling tip and sample (see refs 43 and 44 for further details).

3. RESULTS AND DISCUSSION

In order to fully characterize the perylene adsorption on the $\text{TiO}_2(110)-(1 \times 1)$ surface we studied samples with different molecular coverages, ranging from 0.3 to 1 ML. Figure 1 shows STM images comparing the low (top panel) and high (bottom panel) coverage regimes. In the first case, both individual molecules and the rows of the substrate in the uncovered regions are clearly observed. Perylene appears as an elongated feature with the long axis oriented parallel to the [001] crystallographic direction. Besides, it is well-known that the bright rows observed by STM at positive voltages (applied to the sample) correspond to the Ti rows. A detailed analysis of the STM images shows that, at low coverage, perylene adsorbs

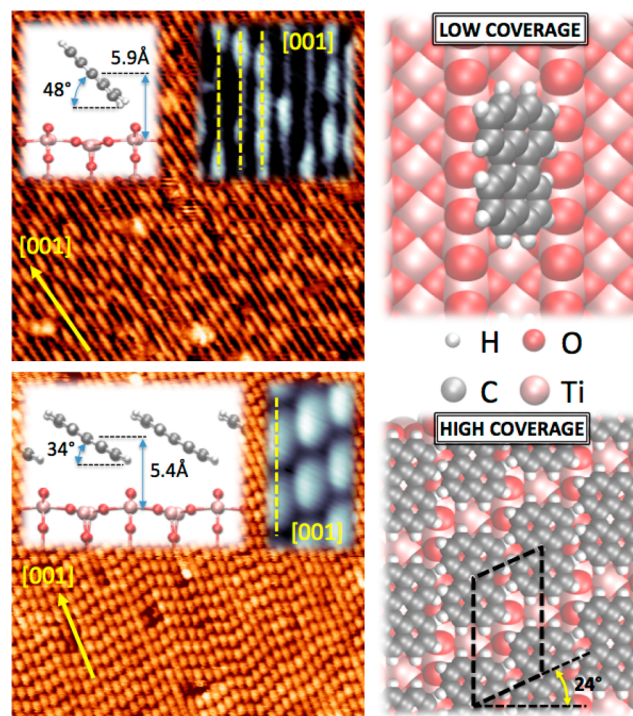


Figure 1. UHV-STM images for low coverage (top panels) and high coverage (bottom panels) of perylene molecules on the $\text{TiO}_2(110)-(1 \times 1)$ surface. Yellow lines indicate the [001] directions. For a better visualization, enlarged details of the UHV-STM images, as well as side view of the ball and stick geometrical models, are shown as insets in left panels. Right panels show top views of the ball geometrical models, indicating the unit cell of the high coverage model (dashed line). Colored STM images: $(20 \times 20) \text{ nm}^2$.

on the Ti rows, i.e., in between O_b rows. This adsorption configuration is at odds with those reported for structurally related perylene derivatives, such as PTCDA²⁰ and PTCDI²¹ that adsorb on the O_b rows, and rather resembles the case of the much narrower acene molecules.^{16,17}

At low coverage, the molecular distribution does not reflect any significant intermolecular interaction, either attractive or repulsive. The adsorption configuration seems to be driven only by the large structural corrugation of the TiO_2 surface associated with the protruding O_b rows. Besides, we observed by STM a large molecular mobility at room temperature, indicating a weak chemical interaction between the molecules and the substrate. Overall, perylene molecules are scattered among the O_b rows like a 2D gas. This weak molecule—substrate and intermolecular interaction, with no subtle chemistry underlying—is in full agreement with previous works performed for high coverages samples based on XPS, UPS, and NEXAFS.^{18,45}

Neglecting the movement of the molecules during the data acquisition, and by a statistical analysis over hundreds of molecules, we obtain values of 3.7 \AA for the molecular width, 11 \AA for the length and, by taking the Ti rows as a reference, 1 \AA for the height. As the coverage is increased toward the monolayer limit (bottom panels of Figure 1), the perylene adsorption structure drastically changes. We observed the onset of a significant *side-to-side* as well as *head-to-head* molecular attraction yielding the formation of compact ordered domains. We remark that whenever we tried to increase the molecular coverage by deposition at room temperature (with the same

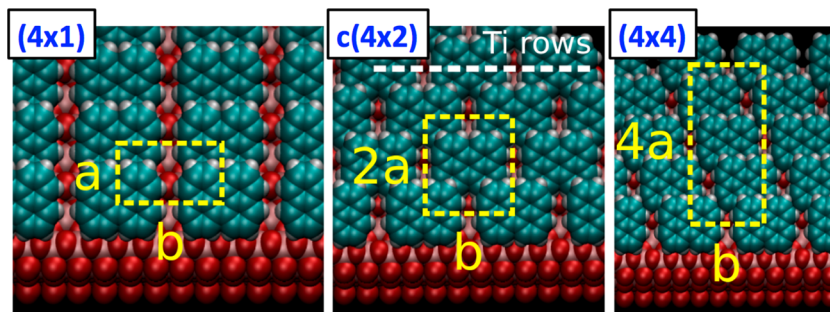


Figure 2. Ball-model pictorial schemes of the three inequivalent geometrical configurations for the high coverage regime perylene/TiO₂(110) phase fitting the experimental evidence used in the calculations. Dashed yellow lines represent the unit cell of the different models, where $\mathbf{a} = 6.6 \text{ \AA}$ and $\mathbf{b} = 11.9 \text{ \AA}$. Ti rows [001] direction is represented by a white dashed line.

low rates) always produced samples like that in left-bottom panel of Figure 1. This indicates that 1 ML is the saturation coverage at room temperature, likely due to a decrease of the sticking coefficient due to the structural mismatch between the molecular overlayer and the perylene crystalline packing.

The unit cell in the high-density condensed phase follows two orientations with respect to the main crystallographic directions of the substrate. The first one is parallel to [001], with a molecular spacing of about 1.2 nm, which is consistent with a 4-fold periodicity along the O_b rows ($\sim 1.18 \text{ nm}$). The second one is at 24° with respect to the [1–10] direction (see bottom panel of Figure 1), and the distance between consecutive molecules in this case is of 0.75 nm. With this information, the unit cell of the perylene superlattice can be described by the matrix $\mathbf{A} = \begin{pmatrix} 1 & 1 \\ 0 & 4 \end{pmatrix}$ with respect to the substrate. At the same time, we detected the expected domains in which the molecules arrange following the specular reflection with respect to the [001] direction, described by the matrix $\mathbf{B} = \begin{pmatrix} 1 & 1 \\ 0 & 4 \end{pmatrix}$.

A noticeable difference between the low and high coverage STM images (see Figure 1) is the width of the elongated ovals. In the first case, it is 3.7 \AA while in the last case it is about 5 \AA . In the case of low coverage regime, we mostly detect isolated oval features; therefore, each bright protrusion can be confidently associated with a single molecule. In the monolayer regime the interaction between neighboring molecules can contribute substantially to the STM signal, hampering a simple interpretation of the corresponding images (as shown in the left-bottom panel of Figure 1), which requires a deeper analysis.

For a better understanding of these structures we carried out DFT+D calculation considering both, low and high coverages. For the first case, we have considered a dilute phase with the support of the available experimental input. For this purpose, a TiO₂(110) surface was modeled in a repeated slab geometry: (i) a slab of four physical TiO₂(110) layers with a minimum distance of $\sim 25 \text{ \AA}$ of vacuum between neighboring cells along the axis perpendicular to the surface; as well as (ii) full periodic boundary conditions representing an infinite TiO₂(110) surface. Each substrate physical layer of oxide contained 60 atoms with perfectly balanced stoichiometry in order to avoid polarization effects. A rectangular cell of $(14.9 \times 13.2) \text{ \AA}^2$ containing a perylene molecule has been used for this low coverage regime, large enough to minimize the interaction between neighboring molecules. The Brillouin zone (BZ) was sampled by means of a $[2 \times 2 \times 1]$ Monkhorst–Pack grid,⁴⁶ guaranteeing a full convergence in energy and electronic

density. According to the experimental data, where perylene molecules adsorb along the Ti rows in the low coverage regime, we have fully relaxed two inequivalent starting configurations: one with the central aromatic ring of the perylene molecule lying “on top” of a Ti atom along the Ti rows and another one with the central aromatic ring lying on a Ti–Ti bridge atom along the Ti rows. The calculations reveal that the perylene molecule is most stable adopting the first configuration, yielding a tilt angle of about 48° off the surface, around the long molecular axis, and with its center of mass lying at a distance of about 5.9 \AA from the Ti rows (see top panel of Figure 1). From the theoretical optimization, the long axis remains parallel to the [001] direction, i.e., to the Ti rows, without any azimuthal reorientation. The adsorption energy and molecule-to-substrate charge transfer for this low regime configuration can be estimated in 2.43 eV and 0.05 e^- per molecule, respectively. DFT+D calculations show, if compared to the results obtained within a conventional DFT framework, that the origin of this interaction is mostly derived from the vdW contribution. This interaction at low-coverage regime is high enough to confine the diffusion of the perylene molecules along the Ti rows, in full agreement with the experimental evidence. Nevertheless, the electrostatic nature of this interaction, and therefore the absence of covalent bonding, does not modify the structure of the molecule as we experimentally observe.

The 2D gas-like behavior of perylene at low coverage is remarkably different from that reported for pentacene, where molecules display a strong *side-to-side* attraction since the early stages of deposition. This effect might be attributed to a different weight of the electronic orbital contribution (i.e., hybridization) to the interaction with respect to the electrostatic forces and to the van der Waals ones. The latter ones are expected to be similar for the two molecules, while there is a different balance between the $\pi-\pi$ and $\sigma-\pi$ interactions due to the different number and structural arrangement of the C–H bonds between perylene and pentacene.⁴⁷ In particular, the stacked coupling of adjacent pentacenes is indicative of a prominent C–H interaction with the adjacent aromatic system. On the contrary, the longitudinally displaced coupling of adjacent perylenes observed in the monolayer range suggests the occurrence of a *side-to-side* $\pi-\pi$ interaction.^{48,49}

For the monolayer phase, we considered three inequivalent configurations, assuming a common 4-fold intermolecular spacing along the [001] direction: (i) the (4×1) and $c(4 \times 2)$ phases (left and central panels of Figure 2, respectively); and (ii) the (4×4) phase (right panel of Figure 2), which is the extended unit cell proposed by the experiments. For this high-

coverage regime, the $\text{TiO}_2(110)$ surface was modeled, as for the previous low-coverage regime, in a repeated slab geometry: (i) a slab of four physical $\text{TiO}_2(110)$ layers with a minimum distance of $\sim 25 \text{ \AA}$ of vacuum between neighboring cells along the axis perpendicular to the surface; as well as (ii) full periodic boundary conditions representing an infinite $\text{TiO}_2(110)$ surface. Each substrate physical layer of oxide contained 24 atoms with perfectly balanced stoichiometry in order to avoid polarization effects. In all the calculations the Brillouin zones (BZ) were sampled by means of a $[2 \times 4 \times 1]$ Monkhorst–Pack grid,⁴⁶ guaranteeing a full convergence in energy and electronic density.

Figure 2 shows top views of the DFT+D optimized structures obtained for the three inequivalent high-coverage phases (with $a = 6.6 \text{ \AA}$ and $b = 11.9 \text{ \AA}$). The perylene molecules show an axial tilt angle ranging between 32° and 34° , in agreement, within the experimental indetermination, with the value of $\sim 26^\circ$ obtained from the NEXAFS technique.¹⁸ Also in these cases, no azimuthal reorientations are obtained from the theoretical optimization, which provides a dense packing of the molecules and manifests a non-negligible molecular interaction along the [001] direction, in good agreement with the experimental data.

We performed a couple of additional tests to check the consistency of the theoretical simulations in comparison with the experiments: (i) all the three configurations have been relaxed with the center of the molecules located on Ti atoms and on Ti–Ti bridges along the [001] direction, yielding a higher stability for those configurations with the central aromatic ring of the molecules on Ti atoms, and (ii) we have carried out extra calculations, doubling the cell size along both the x and y directions, to check the stability of the structures obtained in the simulations. The aim of this test was to allow for the possibility of observing new structural reconstructions. The result of this test revealed no new structural effects with respect to those observed in the minimal unit cells; therefore, in the following, we will use the minimal unit cell in all the calculations with confidence.

The optimized geometries for the (4×4) , (4×1) , and $c(4 \times 2)$ perylene phases show adsorption distances and energies of 5.41 , 5.38 , and 5.43 \AA (measured from the center of mass of each molecule to the Ti rows of the $\text{TiO}_2(110)$ surface), and 2.23 , 2.12 , and 2.15 eV per molecule, respectively. Also, the charge transfers, from the molecule toward the substrate in all the cases, are 0.09 , 0.06 , and 0.08 e^- per molecule, respectively. According to these results, the most stable configuration is the (4×4) phase (see lower panel in Figure 1) in good agreement with the model suggested by the STM experiments. However, the low differences in adsorption energy suggest that locally several of these phases could coexist. This might be the reason for the herringbone appearance in some areas of the surface (see bottom panel of Figure 1).

Thus, regarding the adsorption energy of 2.23 eV , obtained for the most stable configuration at high coverage regime, in comparison with that of 2.43 eV , obtained for the low coverage regime, it is possible to conclude that the effect of the molecular packing tends to increase the intermolecular interaction by reducing the interaction with the surface.

At this point it is important to remark that, compared to the conventional DFT results, the inclusion of the vdW interaction parametrization increases—in both low and high coverage regimes—the adsorption distances by $\sim 0.2 \text{ \AA}$, and the adsorption energies by about 50–55%.

UPS measurements reveal that there is not a net charge transfer between adsorbate and substrate (see Figure 3a), in

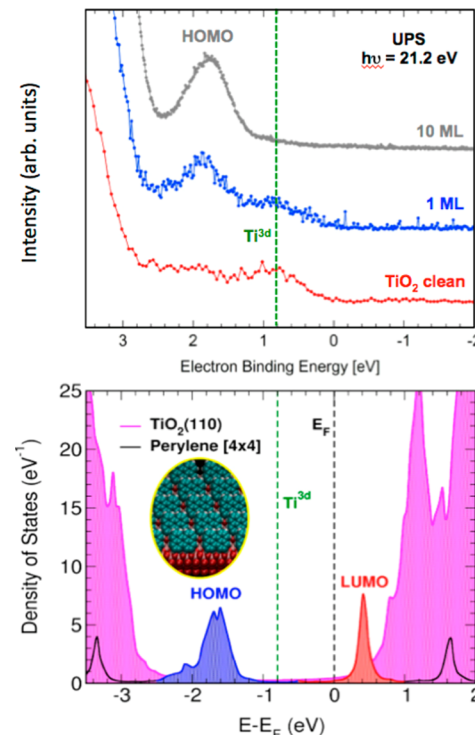


Figure 3. (Top) He-I UPS spectrum (low binding energy region) of the clean $\text{TiO}_2(110)$ surface, 1 ML and a multilayer of perylene. Projected density of states—on both TiO_2 surface and perylene adlayer—for the optimum (4×4) perylene/ $\text{TiO}_2(110)$ interface. For a better comparison, notice that the energy window is the same, and both panels are perfectly aligned with respect to the Fermi level.

good agreement with our theoretical predictions and previous experimental results for both the occupied and unoccupied molecular orbitals.^{18,45} Interestingly, this evidence again relates to the aforementioned finding that perylene adsorbs above the surface mainly by the vdW interaction. Moreover, the dipolar nature of this interaction, and therefore the absence of a proper covalent bonding, does not modify the electronic structure of the molecule as experimentally observed, and reinforced by the UPS analysis.

Once the high-coverage (4×4) phase has been unequivocally associated with the perylene/ $\text{TiO}_2(110)$ ground-state structure by total energy considerations within the DFT+D approach, its electronic structure has been adequately “many-body” corrected, as explained in section 2, by using the GW+BSE formalism implemented in the YAMBO package,²⁷ in order to properly account for the self-energy, electron–hole, and excitonic effects. This accurate framework corrects the transport gap of the molecule in interaction with the substrate with respect to conventional DFT frameworks, and takes into account the surface depolarization, induced interfacial dipoles and image potential effects. More than 200 unoccupied electronic bands were necessary to obtain converged self-consistent results. The electronic structure calculation by GW+BSE of this interface yields an improved transport gap for the perylene molecule on the $\text{TiO}_2(110)$ substrate of 2.2 eV , to be compared with that obtained by standard DFT of 1.4 eV . On the other hand, the band gap

calculated for the $\text{TiO}_2(110)$ surface is 3.6 eV, in excellent agreement with the experimental evidence of 3.5–3.7 eV.⁴

In order to improve the theoretical description of the interface, the available He-I UPS spectroscopic information has been used to correctly align the perylene molecular levels with respect to the TiO_2 substrate electronic bands. The GW+BSE corrected value of the perylene transport gap, as well as the correct alignment of the perylene molecular levels with respect to the substrate, have been included in the localized-basis set FIREBALL code by means of a scissor and a shift operator, respectively (see refs.^{28,35,36} and references therein).

Top panel of Figure 3 shows the experimental He-I UPS spectrum, measured at low temperature, for the clean $\text{TiO}_2(110)$ surface, 1 ML and a multilayer of perylene. Bottom panel of the same figure shows the projected density of states (PDOS)—on both TiO_2 surface and perylene adlayer—for the optimum (4×4) perylene/ $\text{TiO}_2(110)$ interface once the electronic levels have been properly adjusted. For a better comparison between both graphs, notice that the energy window in both panels is the same. Following this strategy, which has provided successful results in similar organic/oxide interfaces,¹⁴ the PDOS profile in bottom panel of Figure 3 shows the LUMO of the perylene laying at around 0.5 eV above the Fermi level, and closely pinning the conduction band of the TiO_2 . This result will be of paramount importance for obtaining accurate simulations of the STM images just at the same tunnelling bias used in the experiment. On the other hand, the HOMO feature appears at about 2 eV below Fermi and the energy position is not depending on the perylene coverage. This fact indicates that the perylene/ TiO_2 interface do not present interface states and both organic layer and substrate are electronically decoupled.

Figure 4 shows a comparison between the experimental and simulated STM images for both the low (left panels) and high (right panels) coverage regimes, at constant-current tunnelling conditions of $I_{\text{tunnel}} = 0.1$ nA, and integrated up to a tunnelling bias of $V_s = 1.4$ V. The agreement between the experimental and theoretical images is remarkable, which substantially enforces the assignment of the (4×4) perylene/ TiO_2 phase as ground-state configuration. Both theoretical and experimental images match not only the morphology of the image, but also the relative intensity of the STM signal. Additionally, according to the calculated DOS profiles shown in bottom panel of Figure 3, the scanning sessions at $V_s = 1.4$ V seem to capture the LUMO of the perylene molecules, which is clearly located in the theoretical DOS profiles around 0.5 eV above the Fermi energy, which is the reference scanning energy.

One of the main advantages of the efficient first-principles strategy adopted here is that we can directly superimpose the structure of the molecules over the simulated STM images in order to properly associate the observed contrast features with the molecular structure (see Figure 4). In the high-coverage phase, corresponding to the (4×4) perylene/ TiO_2 superlattice (right panel of Figure 4), the characteristic oval features appear between the molecules, and therefore the STM intensity seem to have their origin in the *side-to-side* intermolecular hybridization, between the lower region of a molecule with the upper region of the lower part of the neighboring molecule (see right panel in Figure 4, and lower panel of Figure 1). Thus, the bright protrusions observed at high coverages in the experimental STM images are not located along the line connecting the centers of the molecules, i.e., on the Ti rows. On the contrary, the STM bumps are located between neighboring molecules.

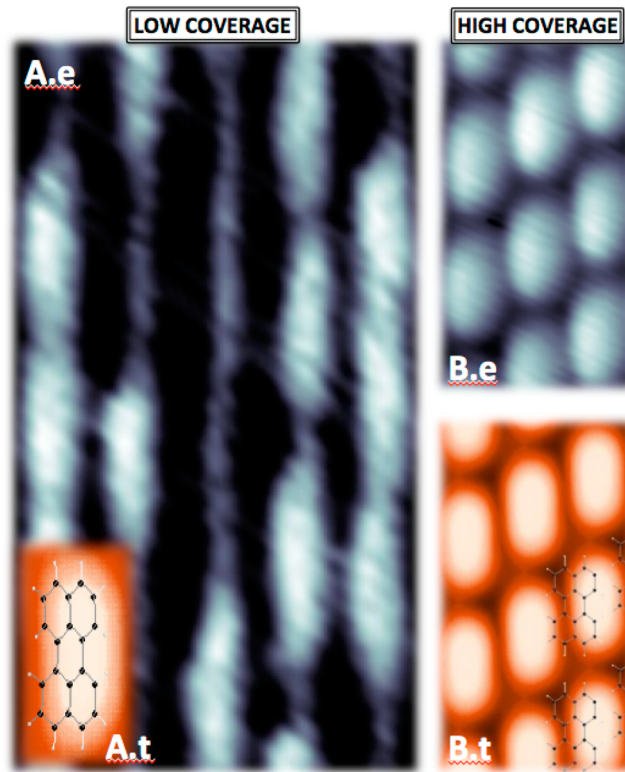


Figure 4. UHV-STM image recorded in constant current mode at $I_{\text{tunnel}} = 0.1$ nA and $V_s = 1.4$ V for the perylene/ $\text{TiO}_2(110)$ at low-coverage regime (panel A.e.) and for the (4×4) ground state perylene/ $\text{TiO}_2(110)$ phase at the monolayer coverage regime (panel B.e.). Simulated STM image at low-coverage regime (panel A.t.) and for the (4×4) ground state perylene/ $\text{TiO}_2(110)$ phase at the monolayer coverage regime (panel B.t.). Theoretical STM images have been simulated under the same scanning conditions than in the experiment. Ball-and-stick perylene geometries have been superimposed on the simulated STM images.

This theoretical result explains the change in the width of the molecules detected in the experimental STM images by comparing low and high coverage regimes (Figure 1 and 4).

We have shown up to now that the (4×4) phase is electronically decoupled from the substrate. Moreover, in order to show that the characterized molecular layer is a realistic candidate for the designing of new nanodevices we tested its thermal stability. Our results show no changes in the perylene monolayer morphology after heating up to temperatures about 400 K. However, occasionally we detect by STM that a few molecules desorb producing a low quantity of defects in the organic layer.

4. CONCLUSIONS

In conclusion, we have shown, by means of an adequate combination of atomic-resolved STM, UPS and NEXAFS experiments with accurate DFT+vdW-based calculations and efficient theoretical STM imaging approach, that perylene weakly adsorbs on the $\text{TiO}_2(110)$ - (1×1) surface both at low and high coverages. For both coverage regimes, the molecules are accommodated along the Ti rows, i.e., in between O_b rows, with their long axis oriented parallel to the [001] direction, and the molecular plane tilted off the surface. At low coverages each perylene molecule can be clearly identified by the STM signature, characterized by mostly a topographical pattern.

Nevertheless, at high coverage the interaction between molecules is found to be mediated by a strong *side-to-side* intermolecular hybridization, and the STM reflects the strong electronic character arising from that hybridization. UPS spectra is used, in combination with a $G_0W_0 + \text{BSE}$ “many-body” approach, to efficiently correct the conventional DFT framework and to adjust the theoretical molecular gap and the energy level alignment between the organic molecule and the oxide, which results in a binding energy of the LUMO level of around 0.5 eV above the Fermi level. The corrections beyond-DFT implemented in the calculations are additionally used to obtain molecular adsorption energies, charge transfer rates, density of states profiles, and theoretical STM images, in excellent agreement with the experimental observations.

AUTHOR INFORMATION

Corresponding Author

*(J.A.M.-G.) Telephone: +34 913349087. E-mail: gago@icmm.csic.es.

Present Addresses

[§]Center for Mechanical Technology and Automation (TEMA), University of Aveiro, 3810-193 Aveiro, Portugal.

[†]Laboratory of Molecular Magnetism, Dipartimento di Chimica “Ugo Schiff”, Università degli Studi di Firenze, via della Lastruccia 3, 50019 Sesto Fiorentino (FI), Italy.

Notes

The authors declare no competing financial interests.

ACKNOWLEDGMENTS

We acknowledge financial support from Spanish Grant MAT2011-26534 (MINECO, Spain). J.I.M. acknowledges funding from the CSIC-JAEDOC Fellowship Program, cofunded by the European Social Fund. L.F. and G.L. acknowledge support from the MIUR of Italy through PRIN Project DESCARTES (Grant 2010BNZ3F2).

REFERENCES

- Thomas, A. G.; Syres, K. L. Adsorption of Organic Molecules on Rutile TiO_2 and Anatase TiO_2 Single Crystal Surfaces. *Chem. Soc. Rev.* **2012**, *41*, 4207–4217.
- Liu, L. M.; Li, S. C.; Cheng, H.; Diebold, U.; Selloni, A. Growth and Organization of an Organic Molecular Monolayer on TiO_2 : Catechol on Anatase (101). *J. Am. Chem. Soc.* **2011**, *133*, 7816–7823.
- Roncali, J.; Leriche, P.; Blanchard, P. Molecular Materials for Organic Photovoltaics: Small is Beautiful. *Adv. Mater.* **2014**, *26*, 3821–3838.
- Diebold, U. The Surface Science of Titanium Dioxide. *Surf. Sci. Rep.* **2003**, *48*, 53–229.
- Nicoara, N.; Roman, E.; Gómez-Rodríguez, J. M.; Martín-Gago, J. A.; Méndez, J. Scanning Tunneling and Photoemission Spectroscopies at the PTCDA/Au(111) Interface. *Org. Electron.* **2006**, *7*, 287–294.
- Lindsay, R.; Wander, A.; Ernst, A.; Montanari, B.; Thornton, G.; Harrison, N. M. Revisiting the Surface Structure of $\text{TiO}_2(110)$: A Quantitative Low-Energy Electron Diffraction Study. *Phys. Rev. Lett.* **2005**, *94*, 246102.
- Diebold, U.; Lehman, J.; Mahmoud, T.; Kuhn, M.; Leonardelli, G.; Hebenstreit, W.; Schmid, M.; Varga, P. Intrinsic Defects on a $\text{TiO}_2(110)(1 \times 1)$ Surface and their Reaction with Oxygen: A Scanning Tunneling Microscopy Study. *Surf. Sci.* **1998**, *411*, 137–153.
- Friedrich, M.; Gavrilla, G.; Himcinschi, C.; Kampen, T. U.; Kobitski, A. Y.; Méndez, H.; Salván, G.; Cerrilló, I.; Méndez, J.; Nicoara, N.; et al. Optical Properties and Molecular Orientation in Organic Thin Films. *J. Phys.: Cond. Matt.* **2003**, *15*, S2699–S2718.
- Godlewski, S.; Szymonski, M. Adsorption and Self-Assembly of Large Polycyclic Molecules on the Surfaces of TiO_2 Single Crystals. *Int. J. Mol. Sci.* **2013**, *14*, 2946–2966.
- Palmgren, P.; Nilsson, K.; Yu, S.; Hennles, F.; Angot, T.; Nlebedim, C. I.; Layet, J. M.; Le Lay, G.; Göthelid, M. Strong Interactions in Dye-Sensitized Interfaces. *J. Phys. Chem. C* **2008**, *112*, 5972–5977.
- Yu, S.; Ahmadi, S.; Sun, C.; Adibi, P. T. Z.; Chow, W.; Pietzsch, A.; Göthelid, M. Inhomogeneous Charge Transfer within Monolayer Zinc Phthalocyanine Adsorbed on $\text{TiO}_2(110)$. *J. Chem. Phys.* **2012**, *136*, 154703.
- Schuster, B. E.; Casu, M. B.; Biswas, I.; Hinderhofer, A.; Gerlach, A.; Schreiber, F.; Chassé, T. Role of the Substrate in Electronic structure, Molecular Orientation, and Morphology of Organic Thin Films: Diindenoperylene on Rutile $\text{TiO}_2(110)$. *Phys. Chem. Chem. Phys.* **2009**, *11*, 9000–9004.
- Sánchez-Sánchez, C.; Lanzilotto, V.; González, C.; Verdini, A.; De Andres, P. L.; Floreano, L.; López, M. F.; Martín-Gago, J. A. Weakly Interacting Molecular Layer of Spinning C_{60} Molecules on $\text{TiO}_2(110)$ Surfaces. *Chem.—Eur. J.* **2012**, *18*, 7382–7387.
- Sánchez-Sánchez, C.; Martínez, J. I.; Lanzilotto, V.; Biddau, G.; Gómez-Lor, B.; Pérez, R.; Floreano, L.; López, M. F.; Martín-Gago, J. A. Chemistry and Temperature-assisted Dehydrogenation of $C_{60}\text{H}_{30}$ Molecules on $\text{TiO}_2(110)$ Surfaces. *Nanoscale* **2013**, *5*, 11058–11065.
- Reiß, S.; Krumm, H.; Niklewski, A.; Staemmler, V.; Wöll, C. The Adsorption of Acenes on Rutile $\text{TiO}_2(110)$: A Multi-technique Investigation. *J. Chem. Phys.* **2002**, *116*, 7704–7713.
- Potapenko, D. V.; Choi, N. J.; Osgood, R. M. Adsorption Geometry of Anthracene and 4-Bromobiphenyl on $\text{TiO}_2(110)$ Surfaces. *J. Phys. Chem. C* **2010**, *114*, 19419–19424.
- Lanzilotto, V.; Sánchez-Sánchez, C.; Bavdek, G.; Cvetko, D.; López, M. F.; Martín-Gago, J. A.; Floreano, L. Planar Growth of Pentacene on the Dielectric $\text{TiO}_2(110)$ Surface. *J. Phys. Chem. C* **2011**, *115*, 4664–4672.
- Fratesi, G.; Lanzilotto, V.; Stranges, S.; Alagia, M.; Brivio, G. P.; Floreano, L. High-resolution NEXAFS of Perylene and PTCDI: A Surface Science Approach to Molecular Orbital Analysis. *Phys. Chem. Chem. Phys.* **2014**, *16*, 14834–14844.
- Stohr, J. *NEXAFS spectroscopy*; Springer-Verlag: Berlin, 1992; Paragraph 9.4.2.
- Godlewski, S.; Tekiel, A.; Piskorz, W.; Zasada, F.; Prauzner-Bechcicki, J. S.; Sojka, Z.; Szymonski, M. Supramolecular Ordering of PTCDA Molecules: The Key Role of Dispersion Forces in an Unusual Transition from Physisorbed into Chemisorbed State. *ACS Nano* **2012**, *6*, 8536–8545.
- Lanzilotto, V.; Lovat, G.; Otero, G.; Sánchez, L.; López, M. F.; Méndez, J.; Martín-Gago, J. A.; Bavdek, G.; Floreano, L. Commensurate Growth of Densely Packed PTCDI Islands on the Rutile $\text{TiO}_2(110)$ Surface. *J. Phys. Chem. C* **2013**, *117*, 12639–12647.
- Lanzilotto, V.; Lovat, G.; Fratesi, G.; Bavdek, G.; Brivio, G. P.; Floreano, L. $\text{TiO}_2(110)$ Charge Donation to an Extended π -Conjugated Molecule. *J. Phys. Chem. Lett.* **2015**, *6*, 308–313.
- Horcas, I.; Fernández, R.; Gómez-Rodríguez, J. M.; Colchero, J.; Gómez-Herrero, J.; Baró, A. M. WSXM: A Software for Scanning Probe Microscopy and a Tool for Nanotechnology. *Rev. Sci. Instrum.* **2007**, *78*, 013705.
- Floreano, L.; Cossaro, A.; Gotter, R.; Verdini, A.; Bavdek, G.; Evangelista, F.; Ruocco, A.; Morgante, A.; Cvetko, D. Periodic Arrays of Cu-Phthalocyanine Chains on Au(110). *J. Phys. Chem. C* **2008**, *112*, 10794–10802.
- Pinardi, A. L.; Otero-Irurueta, G.; Palacio, I.; Martínez, J. I.; Sánchez-Sánchez, C.; Tello, M.; Rogero, C.; Cossaro, A.; Preobrajenski, A.; Gómez-Lor, B.; et al. Tailored Formation of N-Doped Nanoarchitectures by Diffusion-Controlled on-Surface (Cyclo)Dehydrogenation of Heteroaromatics. *ACS Nano* **2013**, *7*, 3676–3684.
- Giannozzi, P.; Baroni, S.; Bonini, N.; Calandra, M.; Car, R.; Cavazzoni, C.; Ceresoli, D.; Chiarotti, G. L.; Cococcioni, M.; Dabo, I.; et al. QUANTUM ESPRESSO: a modular and open-source software

- project for quantum simulations of materials. *J. Phys.: Condens. Matter* **2009**, *21*, 395502.
- (27) Marini, A.; Hogan, C.; Grüning, M.; Varsano, D. YAMBO: An Ab-initio Tool for Excited State Calculations. *Comput. Phys. Commun.* **2009**, *180*, 1392–1403.
- (28) Lewis, J. P.; Jelínek, P.; Ortega, J.; Demkov, A. A.; Trabada, D. G.; Haycock, B.; Wang, H.; Adams, G.; Tomfohr, J. K.; Abad, E.; et al. Advances and Applications in the FIREBALL *Ab-initio* Tight-binding Molecular-dynamics Formalism. *Phys. Status Solidi B* **2011**, *248*, 1989–2007.
- (29) Grimme, S. Semiempirical GGA-type Density Functional Constructed with a Long-range Dispersion Correction. *J. Comput. Chem.* **2006**, *27*, 1787–1799.
- (30) Zhang, Y.; Yang, W. Comment on “Generalized Gradient Approximation Made Simple. *Phys. Rev. Lett.* **1998**, *80*, 890.
- (31) Barone, V.; Casarin, M.; Forrer, D.; Pavone, M.; Sambi, M.; Vittadini, A. Role and Effective Treatment of Dispersive Forces in Materials: Polyethylene and Graphite Crystals as Test Cases. *J. Comput. Chem.* **2009**, *30*, 934–939.
- (32) Vanderbilt, D. Soft Self-consistent Pseudopotentials in a Generalized Eigenvalue Formalism. *Phys. Rev. B* **1990**, *41*, 7892–7895.
- (33) Mowbray, D. J.; Martínez, J. I.; García-Lastra, J. M.; Thygesen, K. S.; Jacobsen, K. W. J. Stability and Electronic Properties of TiO₂ Nanostructures with and without B and N Doping. *J. Phys. Chem. C* **2009**, *113*, 12301–12308.
- (34) Martínez, J. I.; García-Lastra, J. M.; López, M. J.; Alonso, J. A. Optical to Ultraviolet Spectra of Sandwiches of Benzene and Transition Metal Atoms: Time-dependent Density Functional Theory and Many-body Calculations. *J. Chem. Phys.* **2010**, *132*, 044314.
- (35) Martínez, J. I.; Abad, E.; Flores, F.; Ortega, J. Simulating the Organic-molecule/Metal Interface TCNQ/Au(111). *Phys. Status Solidi B* **2011**, *248*, 2044–2049.
- (36) Martínez, J. I.; Abad, E.; Flores, F.; Ortega, J.; Brocks, G. Barrier Height Formation for the PTCDA/Au(111) Interface. *Chem. Phys.* **2011**, *390*, 14–19.
- (37) Hybertsen, M. S.; Louie, S. G. First-Principles Theory of Quasiparticles: Calculation of Band Gaps in Semiconductors and Insulators. *Phys. Rev. Lett.* **1985**, *55*, 1418.
- (38) Hybertsen, M. S.; Louie, S. G. Electron Correlation in Semiconductors and Insulators: Band Gaps and Quasiparticle Energies. *Phys. Rev. B* **1986**, *34*, 5390–5413.
- (39) Röhlfsing, M.; Louie, S. G. Excitons and Optical Spectrum of the Si(111)-(2 × 1) Surface. *Phys. Rev. Lett.* **1999**, *83*, 856.
- (40) Onida, G.; Reining, L.; Rubio, A. Electronic Excitations: Density-functional versus Many-body Green's-function Approaches. *Rev. Mod. Phys.* **2002**, *74*, 601–659.
- (41) Martínez, J. I.; Abad, E.; Calle-Vallejo, F.; Krowne, C. M.; Alonso, J. A. Tailoring Structural and Electronic Properties of RuO₂ Nanotubes: A Many-body Approach and Electronic Transport. *Phys. Chem. Chem. Phys.* **2013**, *15*, 14715–14722.
- (42) Martínez, J. I.; Abad, E.; González, C.; Flores, F.; Ortega, J. Improvement of Scanning Tunneling Microscopy Resolution with H-Sensitized Tips. *Phys. Rev. Lett.* **2012**, *108*, 246102.
- (43) Blanco, J. M.; González, C.; Jelínek, P.; Ortega, J.; Flores, F.; Pérez, R. First-principles Simulations of STM Images: From Tunneling to the Contact Regime. *Phys. Rev. B* **2004**, *70*, 085405.
- (44) Blanco, J. M.; Flores, F.; Pérez, R. STM-Theory: Image Potential, Chemistry and Surface Relaxation. *Prog. Surf. Sci.* **2006**, *81*, 403–443.
- (45) Simonsen, J. B.; Handke, B.; Li, Z.; Møller, P. J. A Study of the Interaction between Perylene and the TiO₂(110)-(1 × 1) Surface-based on XPS, UPS and NEXAFS Measurements. *Surf. Sci.* **2009**, *603*, 1270–1275.
- (46) Monkhurst, H. J.; Pack, J. D. Special Points for Brillouin-zone Integrations. *Phys. Rev. B* **1976**, *13*, 5188–5192.
- (47) Desiraju, G. R.; Gavezzotti, A. From Molecular to Crystal Structure; Polynuclear Aromatic Hydrocarbons. *J. Chem. Soc., Chem. Commun.* **1989**, *10*, 621–623.
- (48) Grimme, S. Do Special Noncovalent π–π Stacking Interactions Really Exist? *Angew. Chem., Int. Ed.* **2008**, *47*, 3430–3434.
- (49) Martinez, C. R.; Iverson, B. L. Rethinking the Term “π-stacking”. *Chem. Sci.* **2012**, *3*, 2191–2201.